Power Control for Directly Interconnected Airborne Wind Energy Systems

Mahdi Ebrahimi Salari
Centre for Robotics & Intelligent
Systems, University of Limerick
Ireland
mahdi.ebrahimisalari@ul.ie

Joseph Coleman
Centre for Robotics & Intelligent
Systems, University of Limerick
Ireland
joseph.coleman@ul.ie

Cathal O'Donnell
Centre for Robotics & Intelligent
Systems, University of Limerick
Ireland
cathal.w.odonnell@ul.ie

Jakub Osmic
Department of Automation and Robotics,
University of Tuzla
Bosnia and Herzegovina
jakub.osmic@untz.ba

Daniel Toal
Centre for Robotics & Intelligent
Systems, University of Limerick
Ireland
daniel.toal@ul.ie

ABSTRACT

In this paper, a small offshore airborne wind energy (AWE) farm consisting of three non-reversing pumping mode AWE systems is modelled and simulated. The AWE systems are interconnected using the direct interconnection technique. The quality of the generated power is analysed and investigated. Power control strategies are implemented and results discussed, with important implications for AWE power take-off designs.

KEYWORDS

Airborne wind energy, Direct interconnection technique, Load sharing control, Reactive power compensation, Non-reversing pumping mode

1 INTRODUCTION

Airborne wind energy (AWE) is a new approach to access more consistent and stronger winds at higher altitudes than can be reached by conventional wind turbines. So far, different types of AWE systems have been introduced [1]. A non-reversing pumping-mode AWE system is a type of airborne wind energy system which employs a kite or a glider for harnessing wind energy. The kite or glider is tethered to a ground station via a tether drum coupled to a generator and a recovery motor. The operation cycle is divided into two phases: the power phase and the recovery phase. During the power phase, the generator is mechanically coupled to the tether drum and generates electrical power. At the maximum tether length, the operation must be switched to the recovery phase. During the recovery phase, the generator is mechanically bypassed by an overrunning clutch and the

tether drum is reversed by the recovery motor to recover the tether to its initial length [2]. The non-reversing pumping mode AWE system is demonstrated in figure 1 (see [2] for greater detail).
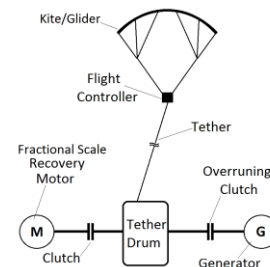

Figure 1: **Simplified schematic of a non-reversing pumping-mode airborne wind energy system**

The direct interconnection technique is utilised for electrical power integration. This technique was first introduced by Pican et al. in 2011 for conventional wind turbines [3]. In this technique, unlike the conventional approach, all the offshore units are directly interconnected to each other without any power electronic converter. After dispatching the power to shore, it is converted in compliance with grid codes by a back to back converter or several paralleled back to back converters. Given that the power electronic converters possess the third highest rate of failure among the wind turbine sub-assemblies [4] and the high maintenance cost of offshore back to back converters, this method could provide a significant increase in the economy and reliability of offshore airborne wind energy systems. The direct interconnection technique and the conventional approach for off-shore power integration are illustrated in figure 2.

Due to the unique method of operation, the power generated by pumping-mode AWE systems is discontinuous. In order to achieve a continuous power output without the use of energy storage systems, an energy farm consisting of a minimum of two units is required. These units must operate in a scheduled sequence defined by a series of time delays implemented between the operation cycles of the individual AWE units. By applying the time delay, the power shortage caused by generators in recovery phase is compensated by other generators. In this condition, other generators in the farm increase their generated power to meet the required power by the load and avoid a power drop. The contribution of each generator in power generation must be proportional to its capacity. Given that the generators in this research are similar, the load must be divided equally between the generators. Otherwise, according to the Millman theorem, since the paralleled generators have the natural tendency to remain synchronised, any load imbalance can cause a large current inconsistency or circulating current between generators [5]. In addition, unequal contribution in the power generation may load a generator more than its nominal capacity. Such extra load can be harmful to the overloaded generator and can lead to generator pole-slipping. In a pole-slipping condition, the synchronous machine has reached its maximum electromagnetic force for staying synchronised with the bus. If a generator becomes loaded more than its maximum capacity, it may lose its ability to keep the rotor synchronised with the stator. Pole-slipping can be very harmful to the generator and the prime mover by causing severe transient torques on the generator shaft [6, 7]. To achieve a continuous power and control the load balance, implementation of a fast and reliable load sharing controller (LSC) is necessary.

When a directly interconnected AWE generator is in the recovery phase, it is mechanically decoupled from the kite recovery operation while the generator is still connected electrically to the main bus. In this condition, the generator operates as an unloaded synchronous motor and needs reactive power exchange to keep the synchronisation with the main bus. This reactive power exchange between the recovery phase AWE and other power phase AWEs increases the power losses in the farm power network through the presence of a circulating

current. The increase in the power loss can be harmful to power network equipment such as generators, transformers, and circuit breakers. Accordingly, utilising a reactive power compensation system can lead to a significant improvement in the quality of the generated power. This paper aims to investigate the power control of the directly interconnected non-reversing pumping mode AWE systems. The interaction of the directly interconnected AWE systems is studied. Furthermore, active power and reactive power of the directly interconnected AWE generators are analysed. In order to control the active power and the load balance, a load sharing controller (LSC) has been developed. The reactive power exchange between the directly interconnected airborne wind energy systems is studied and the implementation of a reactive power compensator (RPC) is examined. Comparing the performance of the directly interconnected non-reversing pumping mode airborne wind energy systems before and after adding the LSC and the RPC to the system shows a significant improvement in the quality of generated power and the performance of the energy farm.
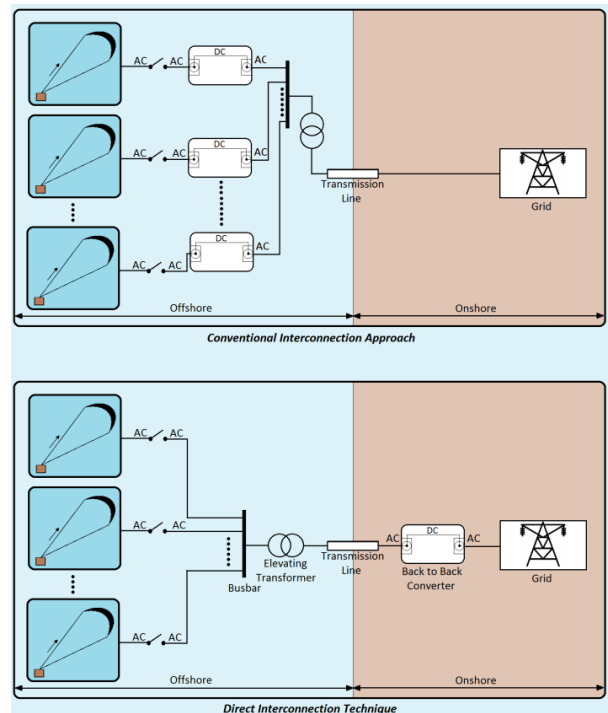

Figure 2: **Conventional approach and direct interconnection technique for off-shore AWE farms.**

2 Simulation Model

The power system diagram of the modelled off-shore AWE farm is illustrated in figure 3. As can be seen, the farm consists of three non-reversing pumping mode AWE systems. In this model, permanent magnet synchronous generators (PMSG) are used as the electrical power take-off. Each AWE system is equipped with an automatic frequency controller (AFC). The AFC in tandem with the kite flight controller attempts to regulate the incoming torque from the kite in order to achieve the operating frequency. The direct interconnection algorithm is demonstrated in figure 4. After reaching the desired frequency, the automatic synchronisation controller (ASC) begins to work. The ASC compares the frequency, voltage amplitude and voltage angle of the generator and the main bus and once they meet the synchronisation criteria it interconnects the corresponding AWE unit with the main bus. Before the interconnection, each system is connected to a local resistive dump load and after the main bus interconnection, the generator is connected to the load along with the other interconnected AWEs. Table 1 shows the specifications of the modelled offshore AWE farm. The nominal frequency of the farm is 18.6 Hz and the operation cycle of AWE systems is 100 seconds with the duty cycle of 80% which means each generation unit operates 80 seconds in the power phase of operation and 20 seconds in the recovery phase of operation. To achieve a continuous power at the main bus a 25 seconds delay between the operations of the generators is implemented.

Table1. Simulated system specifications

PMSG nominal frequency (Hz)	18.6
PMSG flux linkage (Wb)	6.86
PMSG stator resistance (mΩ)	47
PMSG number of pole pairs	45
Dump loads resistance (Ω)	10
Main load resistance (Ω)	3.75
AWE period (s)	100
AWE duty cycle (%)	80
AWE cycle phase delay (s)	25

2.1 Tethered wing and power take-off model

The system speed is governed by the differential equation given by [2]:

$$T_m - T_e - B\omega_r - T_f = J\frac{d\omega_r}{dt} \tag{1}$$

Where T_e is the generator electromagnetic torque, B is the combined viscous friction coefficient of generator rotor and drive, T_f is the drive friction torque and J is the combined inertia of generator and drivetrain.

The speed of the tether drum and the tether are related by (2).

$$V_t = r.\omega_d \tag{2}$$

Where ω_d is the angular velocity of the tether drum, and r is drum radius. The tether drum mechanical torque due to tether force is calculated by:

$$T_m = F_t.r \tag{3}$$

Where F_t is the tether force and it is described in [8]. Since the tether drum is connected directly to the generator, the velocity of the generator rotor is equal to the drum velocity:

$$\omega_d = \omega_r \tag{4}$$

Figure 5 shows the kite torque availability for the generator. The torque is defined as a constant torque with two fluctuating components added to it; a sinusoidal torque representing the periodic maneuver of the wing in the figure of eights and a band limited white noise toque representing the wind turbulence. Due to the lack of large datasets of the kite test results, it is difficult to model torque from the kite more precisely. Comparing the represented torque in figure 5 with the presented results in [1, 9, 10, 11, 12], shows the torque in figure 5 can be considered similar to the torque in experimental systems.
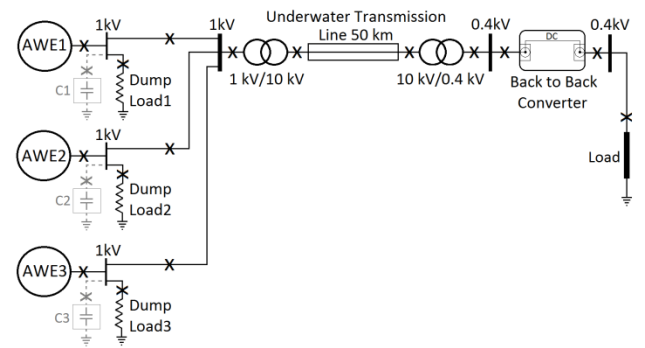

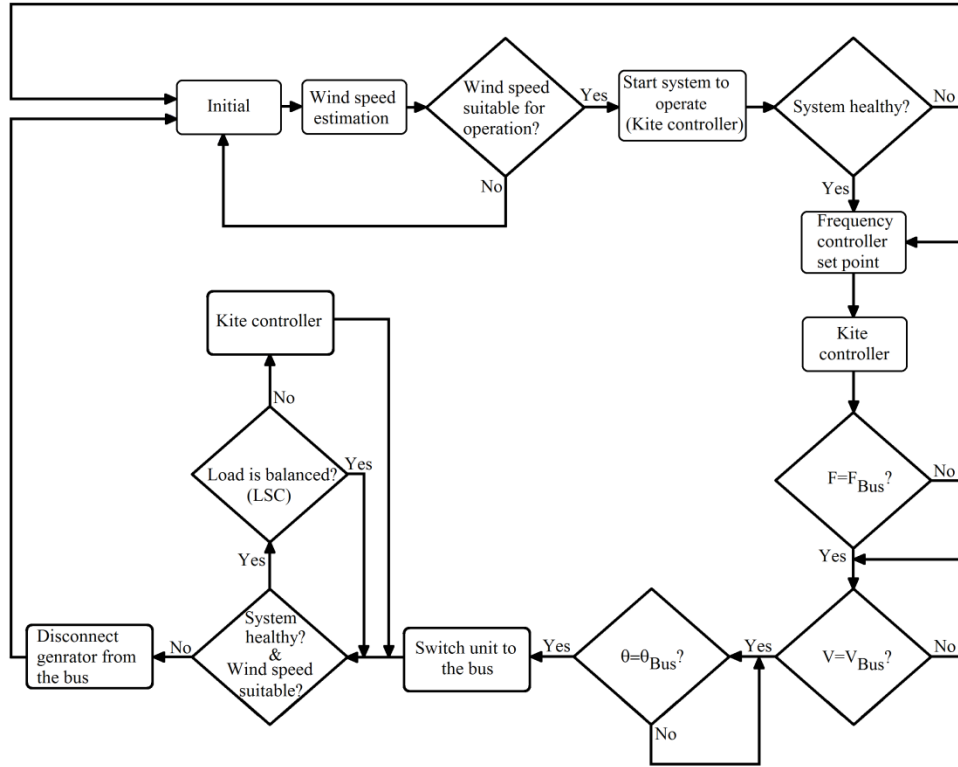Figure 3: **Power system diagram of the simulated offshore non-reversing pumping mode AWE farm**

Figure 4: **Direct interconnection algorithm**

2.2 Permanent Magnet Synchronous Generator Model

The electromagnetic force of a PMSG with round rotor is defined in the rotor d-q reference frame as [3]:

$$T_e = \frac{3}{2} \, n_p . \psi_{PM} . i_{sq} \tag{5}$$

Where n_p is the number of pole pairs, ψ_{PM} is the flux linkage produced by magnets and i_{sq} is the stator current in the d-q reference frame. The internal voltage of the stator windings of the PMSG is calculated by (6).

$$|E| = 2\pi . f_e . \psi_{PM} \tag{6}$$

In (6) f_e is the electrical frequency and is related to the rotor velocity by (7).

$$f_e = \frac{\omega_r . n_p}{2\pi} \tag{7}$$

The stator voltage in the d-q frame is calculated by (8) and (9).

$$u_{sd} = -R_s i_{sd} - 2\pi . f_e \psi_{sq} + \frac{d\psi_{sd}}{dt} \tag{8}$$

$$u_{sq} = -R_s i_{sq} + 2\pi . f_e \psi_{sd} + \frac{d\psi_{sq}}{dt} \tag{9}$$

Where u_{sd} and u_{sq} are the stator terminal voltages, R_s is the stator resistance, i_{sd} and i_{sq} are the stator currents in the d-q frame. The induced flux linkages in the stator are given by (10) and (11).

$$\psi_{sd} = -L_d i_{sd} + \psi_{PM} \tag{10}$$

$$\psi_{sq} = -L_q i_{sq} \tag{11}$$

Where L_d and L_q are the stator inductances. The active and reactive powers of the synchronous generator are given by (12) and (13) respectively.

$$P_{gen} = \frac{3}{2}\left[u_{sd}i_{sd} + u_{sq}i_{sq}\right] \tag{12}$$

$$Q_{gen} = \frac{3}{2}\left[u_{sq}i_{sd} + u_{sd}i_{sq}\right] \tag{13}$$
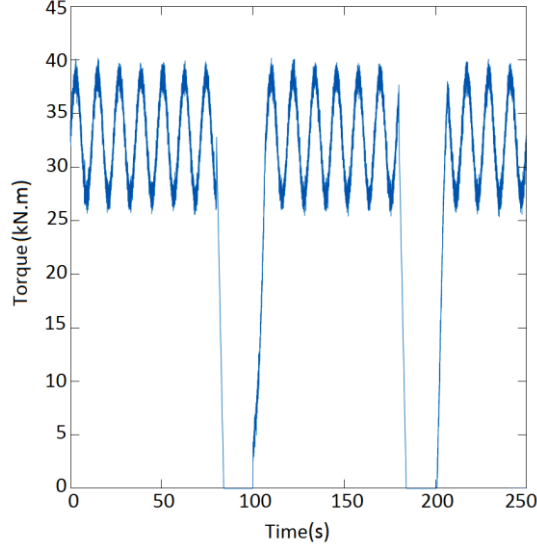
Figure 5: **The available torque from the kite**

3 Simulation results

The frequency of the generators for 500 seconds is demonstrated in figure 6. AWE1 starts to work at $t = 0$ s and AWE2 and AWE3 launch operation with 25 seconds delay at $t = 25$ s and $t = 50$ s respectively. With the operation of each generation unit, the automatic frequency controller and automatic synchronisation controller are activated to prepare the corresponding system for the main bus interconnection. As can be seen in figure 6, AWE2 is integrated to the main bus at $t = 42.03$ s and AWE 3 joins the main bus at $t = 54.39$ s. Since the incoming torque from the wing is highly oscillatory, it is not possible to achieve a constant frequency. However, the AFCs can control the frequency within a reasonable range (less than 6% error) around the operational frequency set point. After interconnecting all generation units to the main bus, the generators are synchronised and one AFC can control the main bus frequency, hence AFC1 is considered as the main bus frequency controller and if AFC1 is in the recovery phase or faulty, AFC2 operates as the backup main bus controller.

The generated power at the main bus is illustrated in figure 7. At start just AWE1 is interconnected with the

main bus and it generates 120 kW electrical power. After the interconnection of AWE2 and AWE3, the electrical power at the main bus is increased to about 235kW and 350 kW respectively. However, while the generated power of each generator is discontinuous, the total power at the main bus is continuous due to the applied time delay between the operations of the AWE systems. According to figure 8, the RMS value of the phase voltage at the main bus is 564 V. The peak value of the main bus voltage is about 810 V.
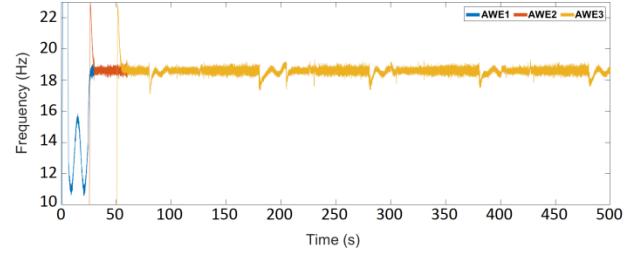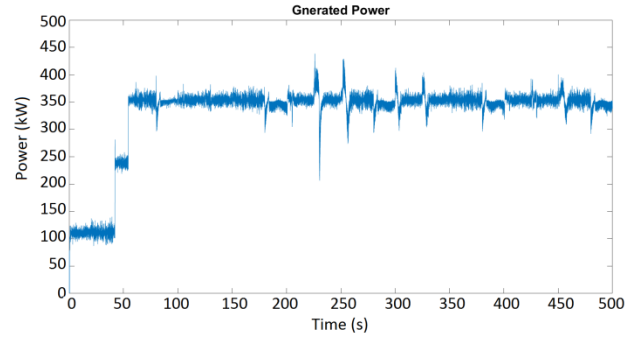
Figure 6: **Generators frequencies**

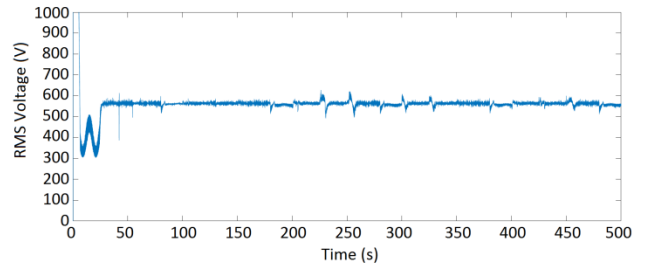Figure 7: **Generated active power of the farm at main bus**

Figure 8: **Main bus voltage**

Figure 9 shows the measured RMS current at the terminals of the generators and the main bus. As can be seen after the interconnection of all generators to the main

bus, total current at the main bus is about 210 A. In figure 9, the power phase of operation and the recovery phase of the operation are determined by green and red colours respectively. When a generation unit operates in the recovery phase, other generators increase their power generation to compensate for the power shortage so that current at the main bus is unchanged and continuous. However, this increase in the power generation is not balanced equally. For instance, between $t = 80$ s and $t = 100$ s when AWE1 is in the recovery phase, AWE2 and AWE3 increase their generated current to around 59 A and 190 A respectively. This uneven increase in power generation can be harmful to the farm power system by increasing the risk of pole slipping and power losses. To keep the load balance in the farm power network a load sharing controller (LSC) has been developed. The control diagram of the farm is illustrated in figure 10. The LSC measures and compares the current at the main bus and the generated current by each interconnected generator. If the LSC detects that a generator is loaded more than other generators in the farm, it tries to correct the generator contribution by regulating the mechanical torque of that generator. The mechanical torque regulation is performed by sending a command signal to the kite controller. Figure 11 demonstrates the generators and the bus currents after adding a load sharing controller. As can be seen, the load is divided equally between the generators. For instance between $t = 80$ s and 100 s when AWE1 is in the recovery phase, the generated current by AWE2 and AWE3 is increased equally. As aforementioned, after interconnection of all generators to the main bus AFC1 operates as the pilot controller in order to control the farm frequency. In the load sharing strategy, AWE1 is the only generation unit which is permitted to generate slightly more (power) than other generators for frequency regulation.

In figures 9 and 11, it can be observed that when an AWE unit is in the recovery phase, it exchanges about 74 A of current with the main bus. This current is due to the reactive power exchange between the recovery phase unit and other generators. During the recovery phase, the generator which is decoupled from the kite and tether drum is still electrically connected to the main bus. In this condition, the permanent magnet synchronous generator operates as an unloaded synchronous motor. This unloaded synchronous motor draws a small amount of

active power and exchanges a significant amount of reactive power to stay synchronised with the other generators. In figure 12, it can be seen that when a unit is in the recovery phase a large amount of reactive power is exchanged with the other generators. As an illustration, between $t = 80$ s and $t = 100$ s, AWE1 is in the recovery phase and it swaps 130 kvar reactive power with the main bus. During the same time, it can be seen that the swapped reactive powers of AWE2 and AWE3 are increased to 65 kvar to response to the required reactive power exchange by AWE1. This reactive power exchange can decrease the power quality of the system by reducing the power factor. In addition, it increases the power losses by increasing the current flow through the system equipment such as transmission lines, generators, transformers and circuit breakers. To compensate the required reactive power a 135 kvar capacitor bank is installed parallel to the terminals of each generator. In figure 3, the capacitor banks are specified by C1, C2, and C3 for AWE 1, AWE 2 and AWE 3 respectively. Once a unit requires reactive power, the adequate shunt capacitors are switched in to the generator terminals in order to achieve the reactive power compensation. In this condition, the reactive power exchange is performed between the generator and its capacitor bank, and therefore the power loss in the farm power network due to reactive power exchanges is significantly decreased.

Figure 13 demonstrates the farm reactive power exchange after adding a shunt capacitor bank at the output of each AWE. As can be seen, when an AWE unit is in the recovery phase, the amount of the exchanged reactive power with the other generators is decreased about 95%. For instance, when AWE1 is in the recovery phase (between $t = 80$ s and 100 s) the exchanged reactive power with AWE2 and AWE3 is insignificant and instead, the required reactive power exchange is compensated by capacitor banks C1 and C2. Similarly, when AWE2 is in the recovery phase the required reactive power is supplied by C1 and C3. Also, any time that AWE3 is in the recovery phase the required reactive power exchange is provided by C1 and C2. Consequently the exchanged reactive power between the generators is decreased significantly. This reactive power compensation can improve the capacity of the farm for providing more active power for the load by decreasing the circulating current inside the farm power network.
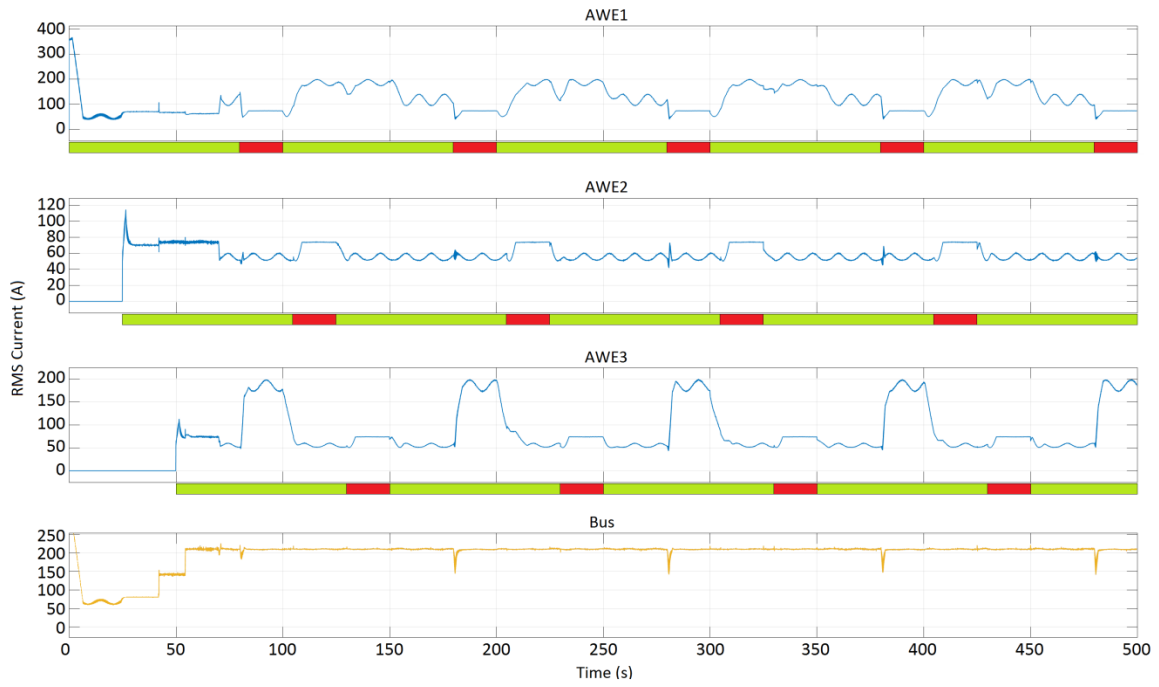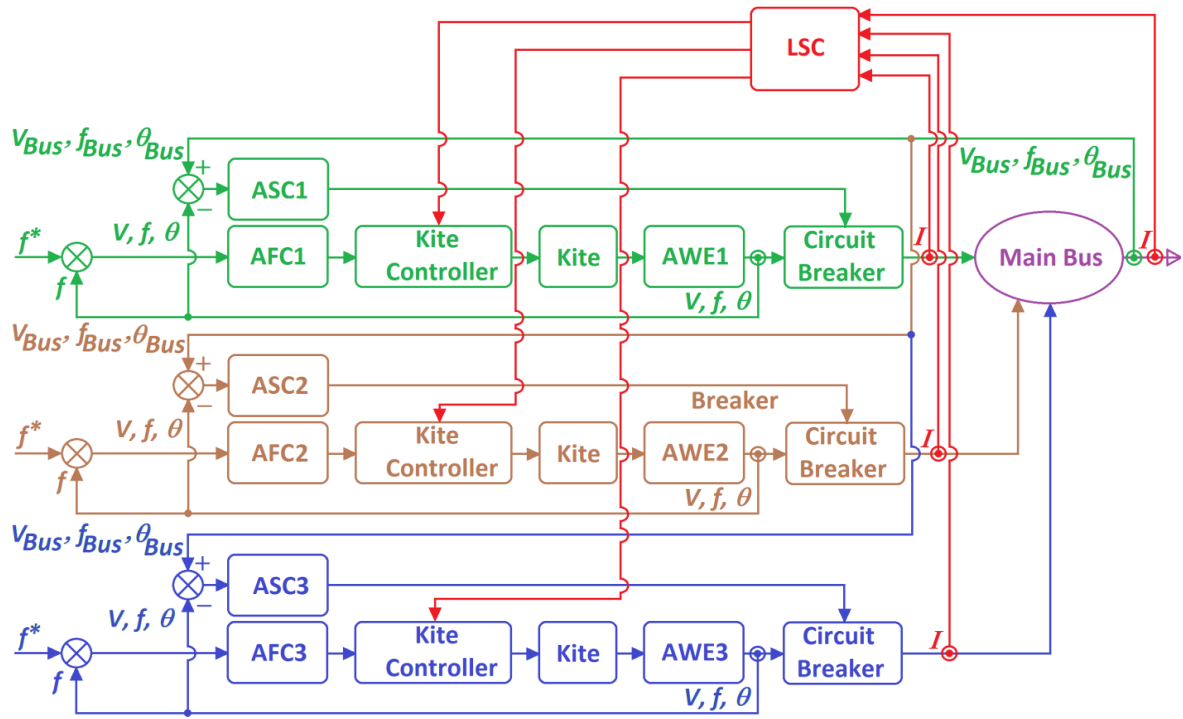
Figure 9: **AWE farm currents**
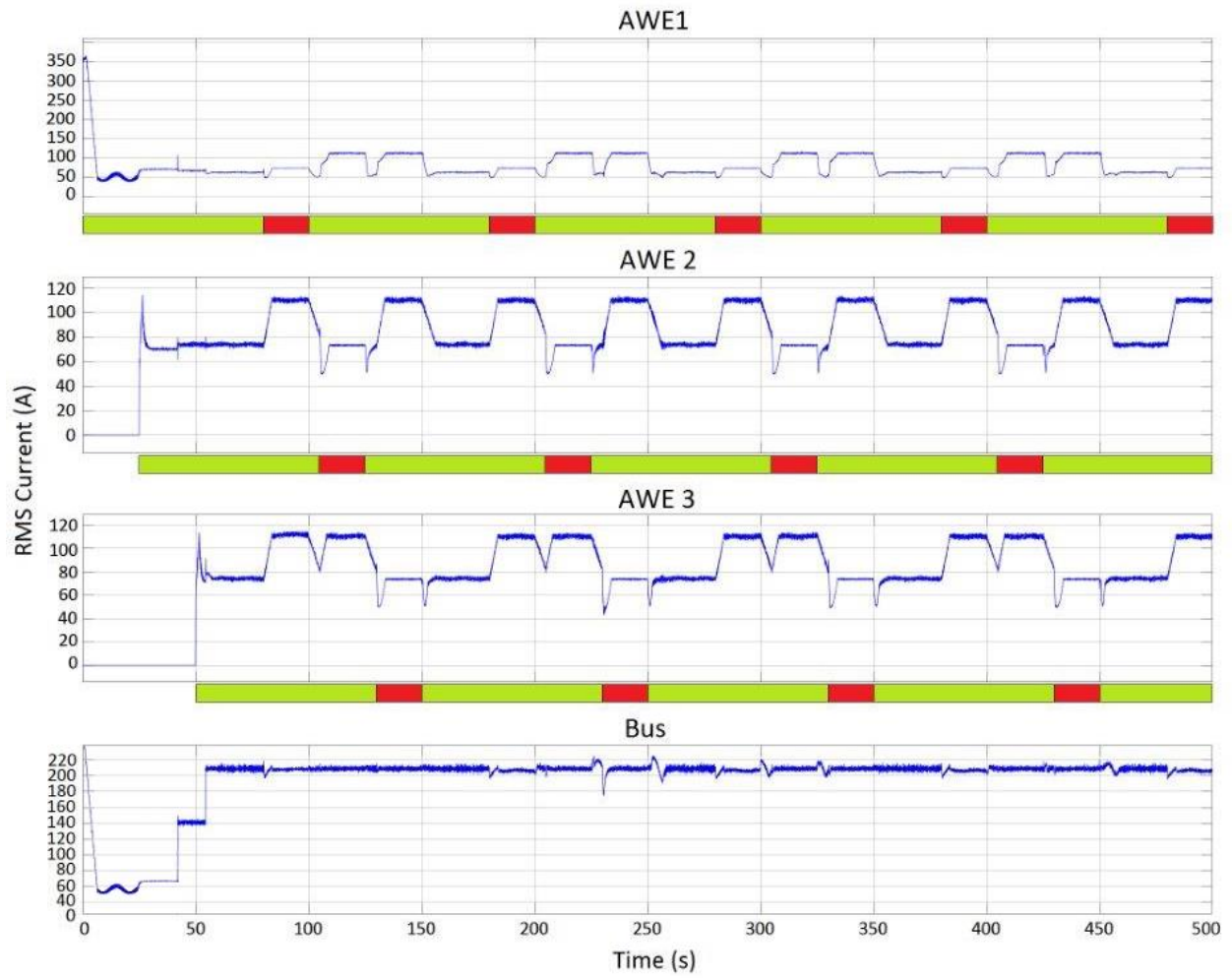

Figure 10: **Control circuit diagram**

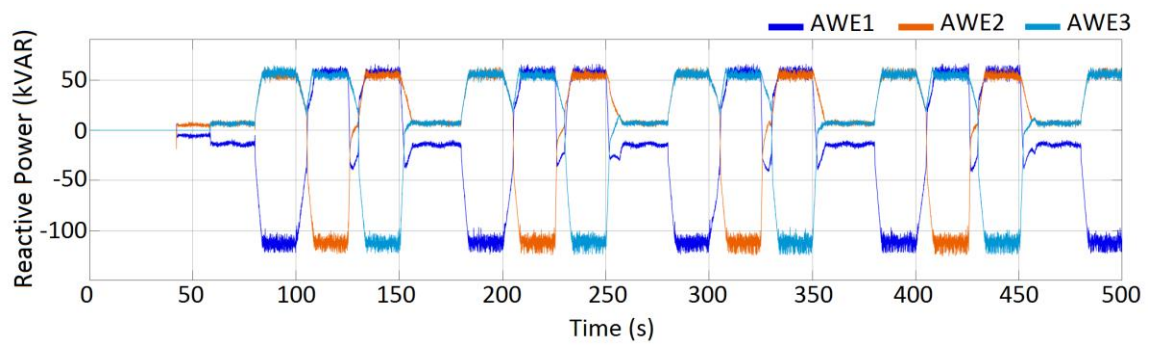Figure 11: **AWE farm currents after adding LSC**

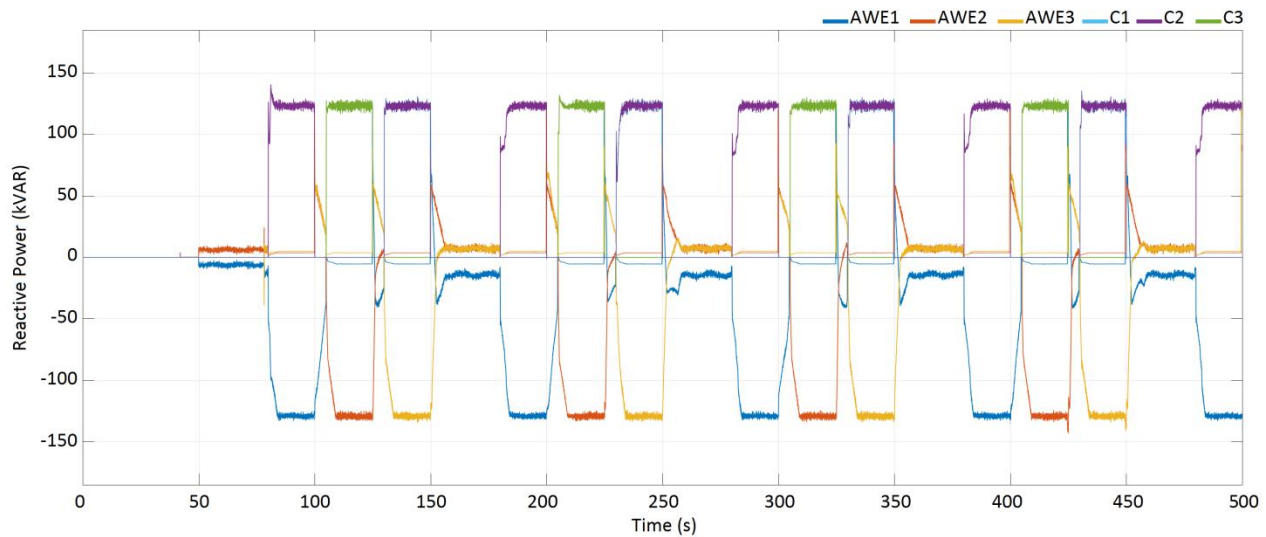

Figure 12: **AWE farm reactive powers**

Figure 13: **AWE farm reactive powers after adding shunt capacitors**

4 CONCLUSIONS

Active and reactive powers of the directly interconnected non-reversing pumping mode AWE systems have been investigated and discussed. It has been shown that without controlling the contribution of each generator in active power generation, the load can be divided unequally between the generators. This uneven load sharing can load a generator more than other generators. It increases the power system losses which can be harmful to the overloaded generator and the network equipment such as transformers, breakers, and capacitors. In addition, the overloaded generator has a high risk of pole slipping and it may cause the farm power network to experience unpredicted power blackouts. A load sharing controller has been designed and implemented to control the load balance and the power generated by each generator. The LSC compares the generated current of each generator and the main bus total current to keep the load in balance. Comparing the generated current by each generator before and after adding an LSC has shown a significant improvement in the farm load flow.

The reactive power exchange between directly interconnected airborne wind energy systems has been analysed. This has shown that when an AWE unit operates in the recovery phase, it swaps a considerable amount of reactive power with the other generators to stay synchronised with them. This reactive power exchange causes a circulating current in the farm power network

leading to increased power losses in transmission lines, transformers, etc. To avoid the negative effects of the reactive power exchange and to improve the power quality, the reactive power must be controlled and compensated. A shunt capacitor bank is installed at the output of each generator to provide the reactive power required by the AWE system during the recovery phase. The reactive power exchange before and after adding capacitor banks have been compared. The simulation results show after adding shunt capacitor banks to control the reactive power exchange; the capacitors rather than the generators have compensated the required reactive power.

Controlling the active and reactive powers is a key factor for improving the reliability and efficiency of the offshore airborne wind energy systems. It can increase the system efficiency by decreasing the amount of circulating current and power losses inside the farm. In addition, controlling the active power to keep the load balance in the farm power network can improve the reliability of the power system by reducing the risk of pole slipping and consequently unpredicted power blackouts.

`

REFERENCES

[1] M. E. Salari, J. Coleman, D. Toal, "Airborne wind energy- a review", In: A. Y. Oral, B. Oral, Z. Banu, editors, 3rd International Congress on Energy Efficiency and Energy Related Materials (ENEFM2015), Springer International Publishing, 2016, 81-92.

[2] J. Coleman, H. Ahmad, E. Pican, D. Toal, "Modeling of a synchronous offshore pumping mode airborne wind energy farm", Energy 71, Elsevier, 2014, 569-578.

[3] Pican E, Omerdic E, Toal D, Leahy M, "Analysis of parallel connected synchronous generators in a novel offshore wind farm model", Energy 36(11), Elsevier, 2011, 6387-6397.

[4] F. Spinato et al, "Reliability of wind turbine subassemblies", IET Renew. Power Gener. 3(4), IET, 2009, 1–15.

[5] M. A. Laughton, D. J. Warne, "Electrical Engineer's Reference Book" Elsevier, chapter 3, 2003 ISBN 9780750646376

[6] G. Klempner, I. Kerszenbaum, "Operation and Maintenance of Large Turbo Generators", John Wiley & Sons, 2004, 27-32 ISBN 0-471-61447-5.

[7] J. Berdy, "Out of Step Protection for Generators" GE Publication No. GER-3179, 1976, 3-26.

[8] R. Schmehl, M. Noom, R. Van der Vlugt, "Traction power generation with tethered wings", In: U. Ahrens, M. Diehl, R. Schmehl, editors, "Airborne Wind Energy", Springer, 2013, 23-46.

[9] R. Van der Vlugt, J. Peschel, R. Schmehl "Design and experimental characterisation of a pumping kite power system", In: U. Ahrens, M. Diehl, R. Schmehl, editors, "Airborne Wind Energy", Springer, 2013, 403-25.

[10] A. Bormann, R. Maximilian, P. Kövesdi, C. Gebhardt, S. Skutnik, "Development of a three-line ground-actuated airborne wind energy converter", In: U. Ahrens, M. Diehl, R. Schmehl editors, "Airborne Wind Energy" Springer, 2013, 427-36.

[11] F. Fritz, "Application of an automated kite system for ship propulsion and power generation", In: U. Ahrens, M. Diehl, R. Schmehl, editors, "Airborne Wind Energy", Springer, 2013, 359-72.

[12] R. Ruiterkamp, S. Sieberling, "Description and preliminary test results of a six degrees of freedom rigid wing pumping system" In: U. Ahrens, M. Diehl, R. Schmehl, editors, "Airborne wind energy" Springer, 2013, 443-58.